

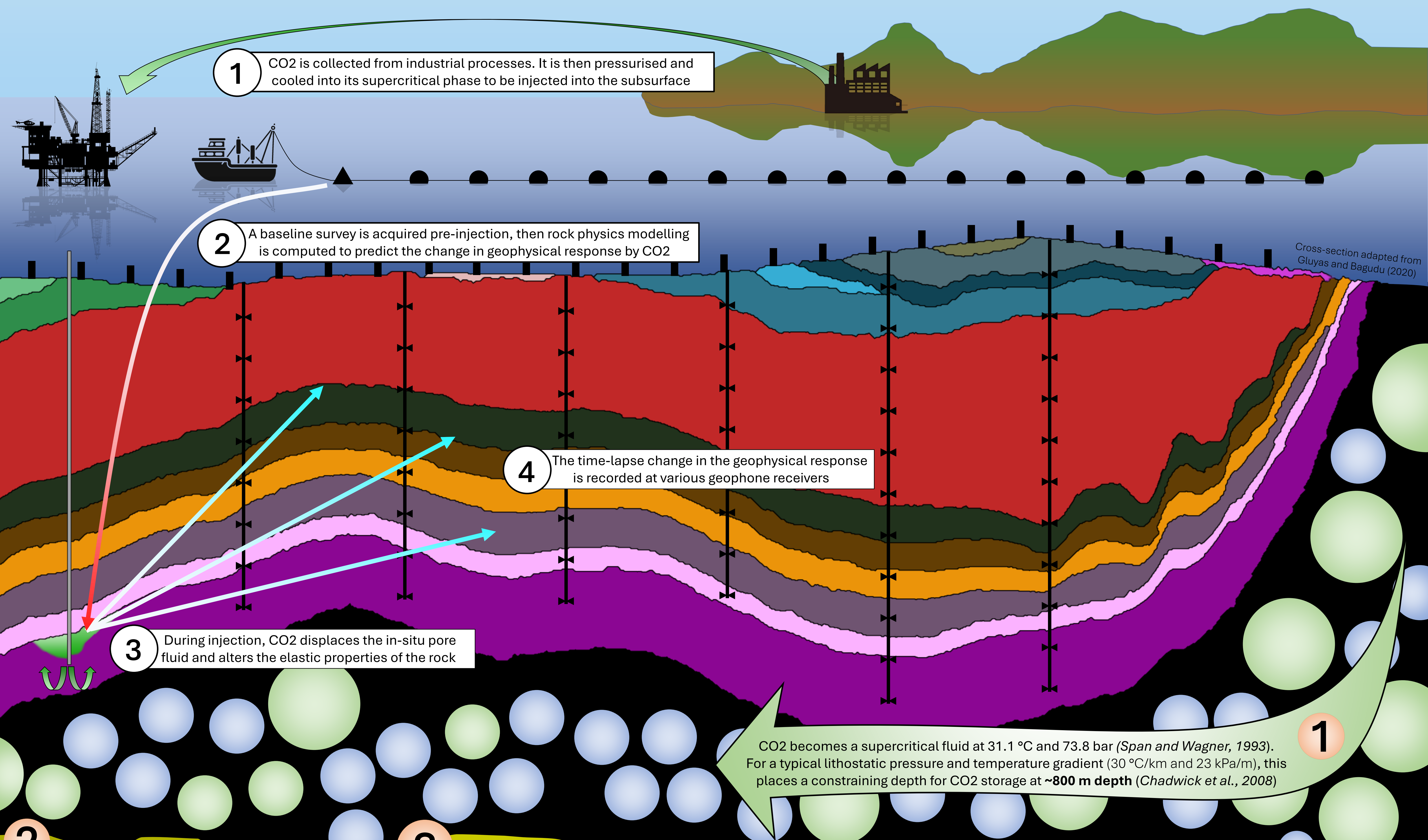
Implication of Non-Gassmann Effects for CO2 Monitoring



THE UNIVERSITY
of EDINBURGH

Martyn Steel^{1*}, Mark Chapman¹, James Verdon² and Rodney Johnston³

¹The University of Edinburgh | ²The University of Bristol | ³BP | * Corresponding author: martyn.steel@ed.ac.uk



- A **baseline** survey is the initial survey acquired before CO2 injection to create a static reservoir model on which simulations are performed
- The **baseline** survey generally consists of a 3D seismic survey and one or more appraisal wells
- The **geophysical response** for this study is considered the seismic attributes relating to seismic travel-time, phase, amplitude and attenuation

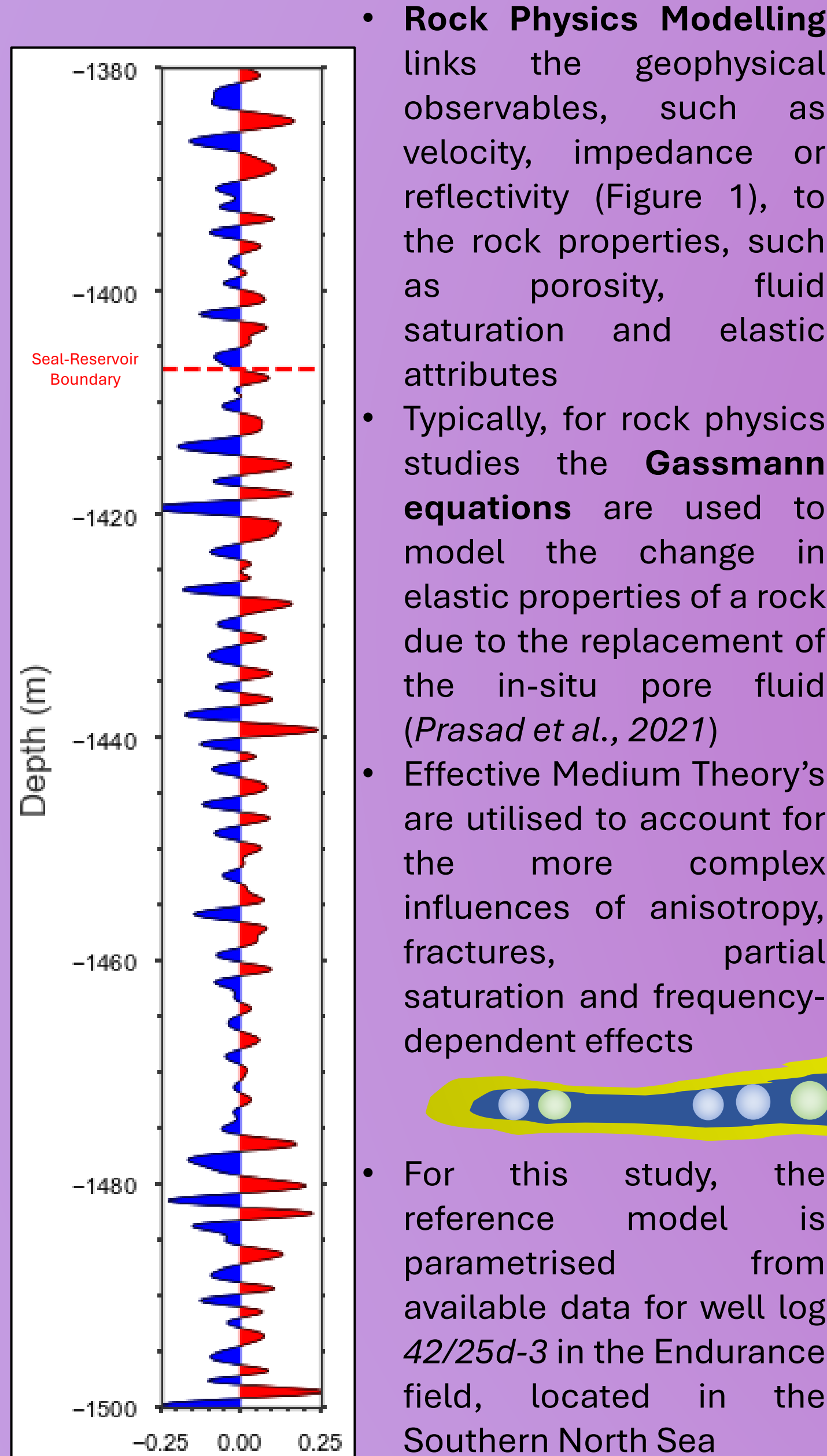


Figure 1: Synthetic seismogram, convolved from well 42/25d-3 derived reflection coefficients with added noise with a 50 Hz Ricker wavelet

Full reference list and acknowledgements available via the QR code.

- Classically, we model the change in the geophysical response using the **Gassmann equations**
- The **Gassmann equations** assume a homogenous, isotropic, linearly elastic, low-frequency rock
- In reality, rocks can be layered, fractured, heterogeneous, non-linearly elastic and multi-frequency

- We propose the use of the **frequency-dependent anisotropic partial saturation model** (Jin et al., 2018), which is an extension of the **Chapman model** (Chapman et al., 2002)

$$C_{ijkl}(\omega) = C_{ijkl}^0(\Lambda, \gamma) - \Phi_P C_{ijkl}^1(\lambda^0, \mu^0, \omega) - \epsilon_C C_{ijkl}^2(\lambda^0, \mu^0, \omega) - \epsilon_f C_{ijkl}^3(\lambda^0, \mu^0, \omega)$$

- This model addresses the limitations of the Gassmann equations (Figures 2 and 3), accounting for the effects of anisotropy (e.g., Hudson, 1980), attenuation (e.g. Ursin and Toverud, 2002), partial saturation (e.g. Papageorgiou and Chapman, 2017) and is consistent with the Gassmann equations in the seismic broadband (10 – 100 Hz) (Mavko et al., 2009) but also consistent with experimental observations in the ultrasonic frequency range (>1 kHz) (e.g. Falcon-Suarez et al., 2020)

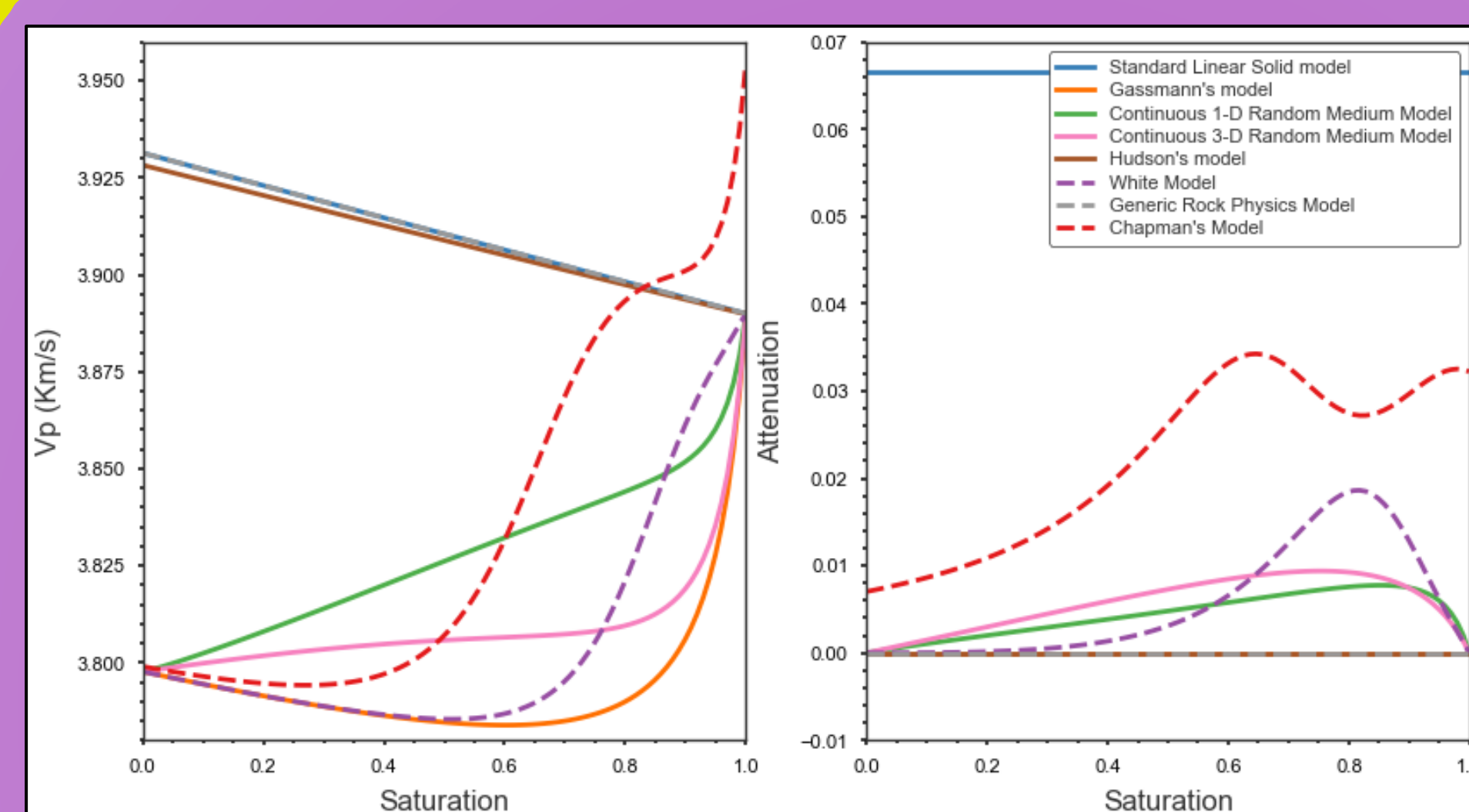


Figure 2: Comparative P-wave velocity (left) and attenuation (right) plots for different rock physics models which account for the effects of saturation, frequency-dependence and anisotropy. The model is defined from the Endurance well 42/25d-3, with the in-situ values of $V_p = 3.89$ km/s, $V_s = 2.18$ km/s, $\rho = 2.31$ g/cm³, and fluid parameters of 0% CO2 saturation, $q = 1$, $T = 40$ °C, $P = 14$ bar and Salinity = 2.6×10^5 ppm (NaCl). Attenuation (right) is calculated by $\text{Im}(C_{1,1}) / \text{Re}(C_{1,1})$.

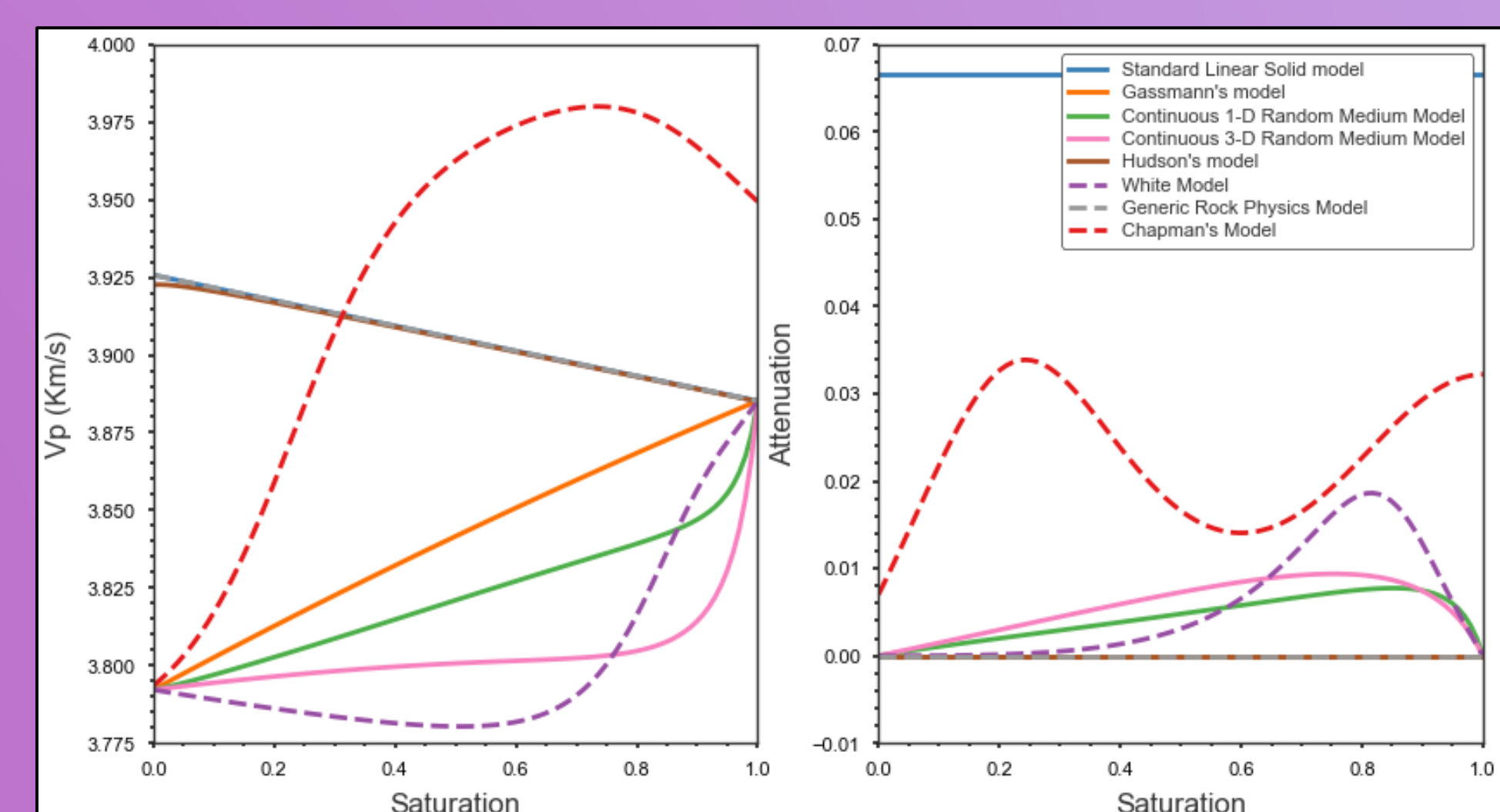


Figure 3: Comparative P-wave velocity (left) and attenuation (right) plots for different rock physics models which account for the effects of saturation, frequency-dependence and anisotropy. The model is similarly parametrised as Figure 2, except with the fluid parameters of 12% CO2 saturation and $q = q_0$.

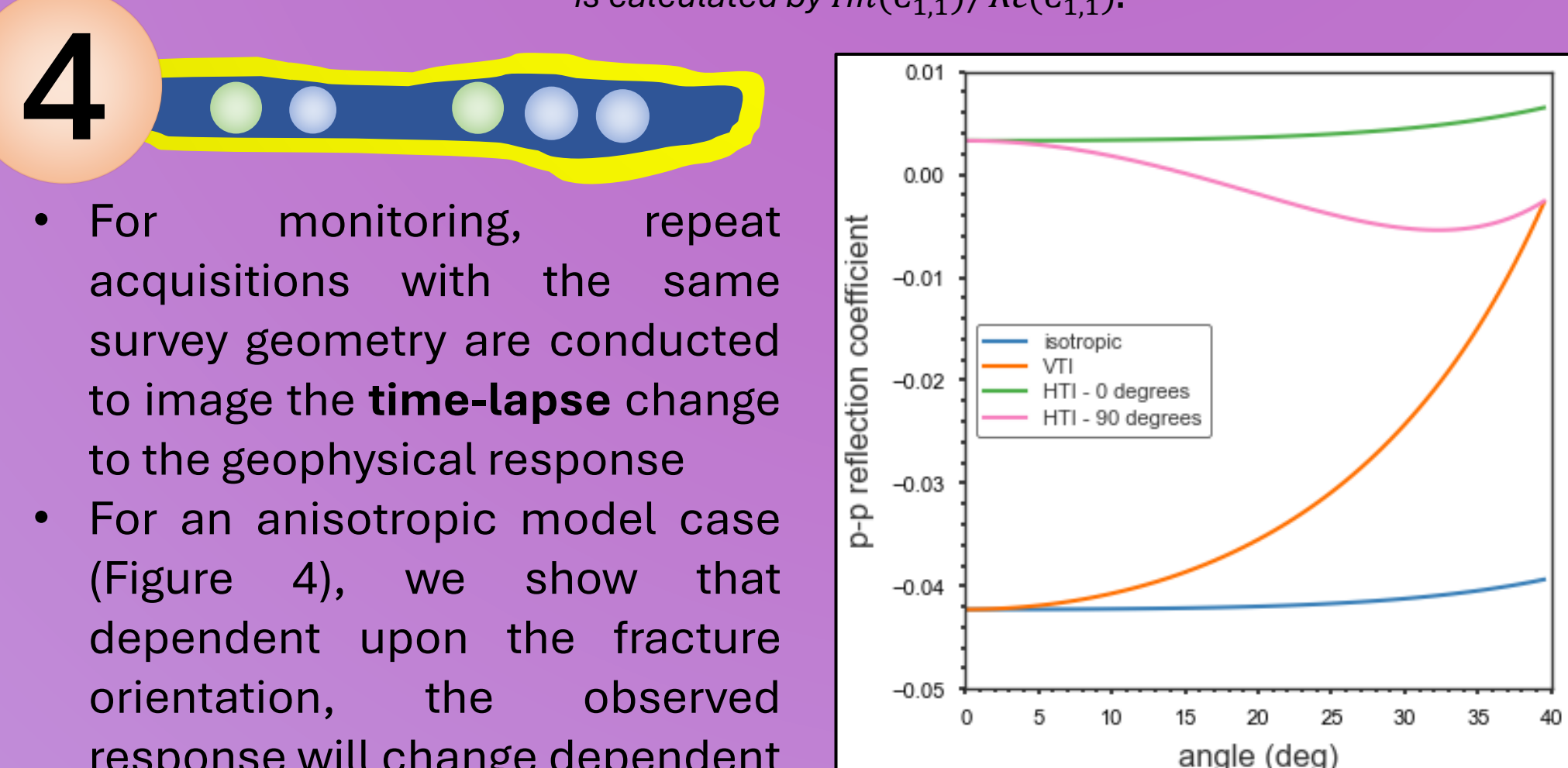


Figure 4: Amplitude Versus Offset (AVO) response using the Schoenberg and Protazio (1990) formulation for different anisotropic media rotations for a model parametrised from Endurance well 42/25d-3

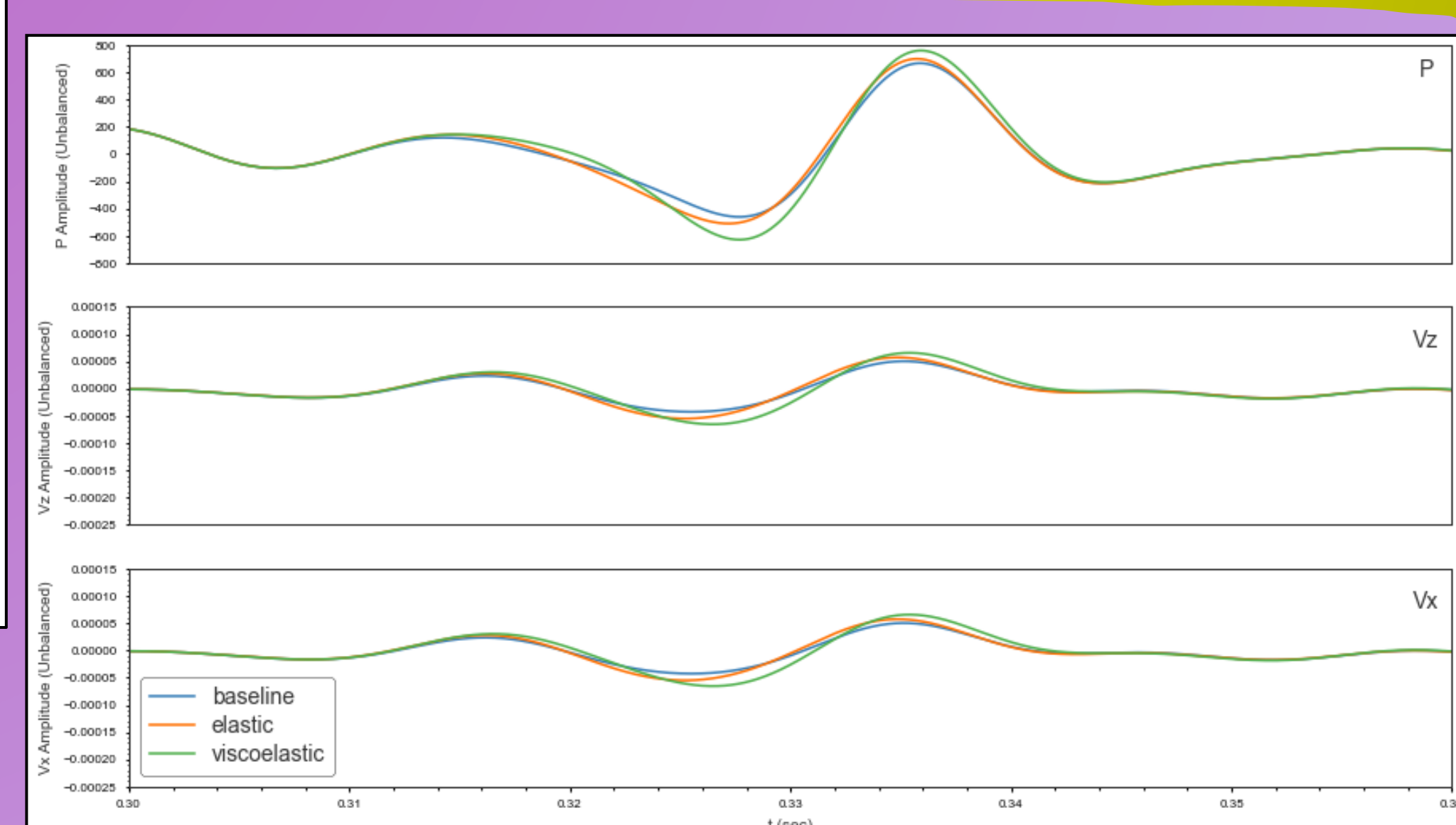


Figure 5: Pressure (top), vertical motion (middle) and horizontal motion (bottom) synthetic Vertical Seismic Profile (VSP) traces generated by staggered-grid, 2D anisotropic viscoelastic finite-difference seismic wavefield simulation. Model is parametrised from Endurance well 42/25d-3 and averaged per lithological formation.

1

CO2 becomes a supercritical fluid at 31.1 °C and 73.8 bar (Span and Wagner, 1993). For a typical lithostatic pressure and temperature gradient (30 °C/km and 23 kPa/m), this places a constraining depth for CO2 storage at ~800 m depth (Chadwick et al., 2008)

1

1

1

1

1

1

1

1

1

1

1

1

1

1

1

1

1

1

1

1

1

1

1

1

1

1

1